Spectroscopic Methods

International Edition: DOI: 10.1002/anie.201700239
German Edition: DOI: 10.1002/ange.201700239

# Ultrafast Independent N–H and N–C Bond Deformation Investigated with Resonant Inelastic X-Ray Scattering

*Sebastian Eckert,* Jesper Norell,* Piter S. Miedema, Martin Beye, Mattis Fondell, Wilson Quevedo, Brian Kennedy, Markus Hantschmann, Annette Pietzsch, Benjamin E. Van Kuiken, Matthew Ross, Michael P. Minitti, Stefan P. Moeller, William F. Schlotter, Munira Khalil, Michael Odelius, and Alexander Föhlisch*

***Abstract:*** *The femtosecond excited-state dynamics following resonant photoexcitation enable the selective deformation of N–H and N–C chemical bonds in 2-thiopyridone in aqueous solution with optical or X-ray pulses. In combination with multiconfigurational quantum-chemical calculations, the orbital-specific electronic structure and its ultrafast dynamics accessed with resonant inelastic X-ray scattering at the N 1s level using synchrotron radiation and the soft X-ray free-electron laser LCLS provide direct evidence for this controlled photoinduced molecular deformation and its ultrashort timescale.*

Ultrafast photoinduced tautomerism and highly directional proton transfers are crucial components of biological photoprotection mechanisms in DNA[1] and melanin.[2–4] In particular, these mechanisms rely on ultrafast energy dissipation in photoinduced proton transfer states[3] that outcompete other energy-dissipating channels. The photoinduced thione–thiol tautomerism in 2-thiopyridone (2-TP), which dominates over the thiol form 2-mercaptopyridine (2-MP) in aqueous solution,[5–8] exhibits an equivalent excited state proton transfer (ESPT) capability in a very compact system.[9] Owing to their common occurrence and functionality, similar thione compounds have become targets for scientific studies of photoexcitation-induced dynamics.[10–14] In these studies, transient optical absorption spectroscopy and computational modeling are combined to reveal details of electronic relaxation pathways, emphasizing in particular the importance of intersystem crossings (ISCs), which were also proposed as possible steps in the photoinduced tautomerism of 2-TP.[9] Herein, the selective and controlled deformation of bonds between the nitrogen atom in 2-TP and neighboring hydrogen and carbon atoms is initiated by resonant photoexcitation. Time-resolved orbital-specific and chemical-state-selective resonant inelastic X-ray scattering[15] (RIXS) at the N 1s X-ray absorption resonance, in combination with first-principle multiconfigurational quantum-chemical calculations, was chosen as a strongly localized probe to observe the initiating processes of the highly directional molecular distortions in photoexcited 2-TP.

The potential energy surfaces (PESs) on which the dynamics of selectively excited 2-TP occur are illustrated in Figure 1a. As will be shown, resonant excitations of 2-TP at different photon energies induce ultrafast dissociation processes of drastically different nature. Excitation from the N 1s core level (X-ray excitation) yields a distortion of the chemical bond between the N atom and the neighboring C atom binding the S atom. In contrast, valence (optical) excitation initiates a deprotonation of the N site.[9] Hence, we utilized the different characteristics of the PESs of the core- and valence-excited (CE/VE) states to induce the deformation of specific bonds in 2-TP.

RIXS has been applied to study the propagation of molecules on both VE-[16] and CE-PESs.[17] Ultrafast proton dynamics in N–H-containing molecules have been observed to complicate the detection of different protonation states.[18] In 2-TP, however, the preference for N–C bond elongation upon N 1s core excitation validates the use of RIXS as a probe for the photoinduced deprotonation process. As shown in Figure 1b, the RIXS process $|i\rangle \rightarrow |t\rangle \rightarrow |f\rangle$ consists of an excitation (X-ray absorption) from an initial state $|i\rangle$ into an intermediate CE state $|t\rangle$, in which the system evolves, followed by a de-excitation (X-ray emission) into a final

[*] S. Eckert, Prof. Dr. A. Föhlisch
Institut für Physik und Astronomie, Universität Potsdam
Karl-Liebknecht-Strasse 24/25, 14476 Potsdam (Germany)
E-mail: sebeckert@uni-potsdam.de
S. Eckert, Dr. P. S. Miedema, Dr. M. Beye, Dr. M. Fondell, Dr. W. Quevedo, Dr. B. Kennedy, M. Hantschmann, Dr. A. Pietzsch, Prof. Dr. A. Föhlisch
Institute for Methods and Instrumentation for Synchrotron Radiation Research
Helmholtz-Zentrum Berlin für Materialien und Energie GmbH
Albert-Einstein-Strasse 15, 12489 Berlin (Germany)
J. Norell, Prof. Dr. M. Odelius
Department of Physics, Stockholm University
AlbaNova University Center, 10691 Stockholm (Sweden)
E-mail: jesper.norell@fysik.su.se
Dr. B. E. Van Kuiken, Dr. M. Ross, Prof. Dr. M. Khalil
Department of Chemistry, University of Washington
Seattle, WA 98195 (USA)
Dr. M. P. Minitti, Dr. S. P. Moeller, Dr. W. F. Schlotter
LCLS, SLAC National Accelerator Laboratory
2575 Sand Hill Road, Menlo Park, CA 94025 (USA)
Supporting information and the ORCID identification number(s) for the author(s) of this article can be found under: http://dx.doi.org/10.1002/anie.201700239.

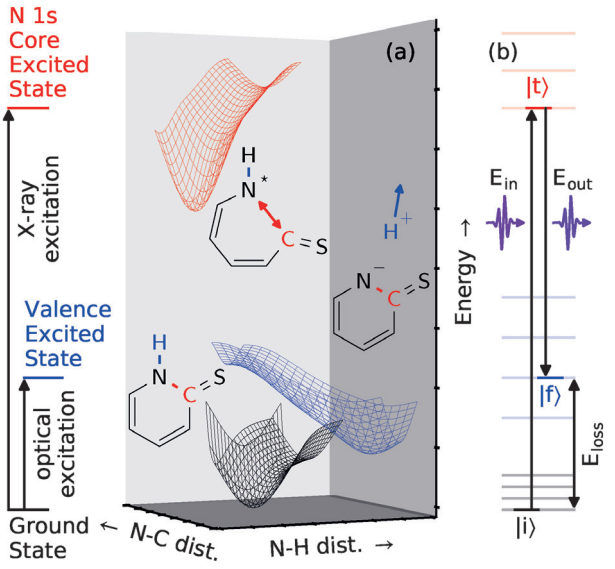


***Figure 1.*** Controlled deformation of bonds in 2-TP by resonant photoexcitation and its visualization. a) Dynamics on excited-state PESs. Selective N deprotonation occurs on the VE-PES (blue) reached by optical excitation from the ground-state PES (black). Bond-cleaving dynamics within the pyridine ring involving the N atom and the sulfur-binding C atom occur on the N 1s core-excited PES (red). b) Excited-state dynamics are detected through the energy loss (difference between the incoming and outgoing photon energy, $E_{loss} = E_{in} - E_{out}$) and transition amplitudes in RIXS measurements. These are affected by (energetic) changes of the initial $|i\rangle$, intermediate $|t\rangle$, and final $|f\rangle$ states of the RIXS process, which in turn result from changes in the orbital occupation and nuclear motion.

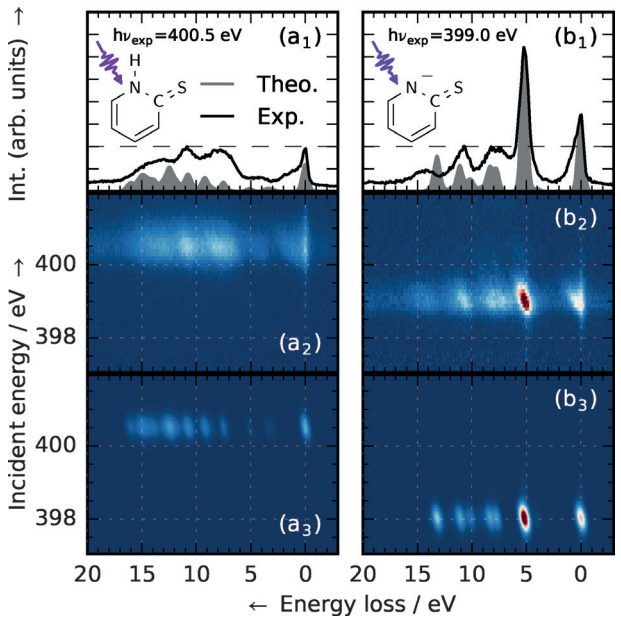


***Figure 2.*** Electronic structure in the N 1s RIXS plane of protonated and deprotonated 2-TP. Left ($a_1$–$a_3$): 2-TP ([2-MP] = 300 mM, thione) in a neutral environment with an absorption resonance energy of 400.5 eV. Integral ($a_1$), experimental ($a_2$), and theoretical ($a_3$) RIXS spectra across the resonance. Right ($b_1$–$b_3$): Deprotonation of 2-TP in a basic environment (2-TP$^-$, [KOH] = 360 mM) with an absorption resonance energy of 399.0 eV. Integral ($b_1$), experimental ($b_2$), and theoretical ($b_3$) RIXS spectra across the resonance. Deprotonation of 2-TP leads to a characteristic red shift of the resonance energy by 1.5 eV and a drastic intensity increase of the spectral line at 5.2 eV energy loss, associated with a N 2p lone pair orbital. The experimental and theoretical spectra and maps were normalized to the intensity of this feature.

(ground or valence-excited) state $|f\rangle$. The emission features depend on the X-ray incident energy and the photon energy loss, and give rise to a two-dimensional spectrum. Signatures of the CE state dynamics can be extracted from the RIXS spectra in the form of broadened and asymmetric line shapes.[19,20] Furthermore, RIXS is sensitive to chemical shifts of X-ray absorption resonances for different molecular species. In the present case, the absorption resonance of the N-deprotonated 2-TP$^-$ species is red-shifted by 1.5 eV relative to that of 2-TP.[8] Hence, RIXS is suitable for studying both the VE-induced deprotonation and the CE dynamics of 2-TP.

RIXS measurements of 2-TP and 2-TP$^-$ (Figure 2$a_{1,2}$ and $b_{1,2}$) were performed at the synchrotron BESSY II to establish characteristic RIXS signatures of the two species. 2-TP$^-$ was stabilized by adjusting the basicity.[8] The RIXS transition intensities of the molecular geometries were simulated on the second order perturbation theory restricted active space level of theory (RASPT2[21,22] in the MOLCAS 8.0 program package;[23] see the Supporting Information) and are shown in Figure 2$a_3$ and $b_3$. The present overestimation of the chemical shift between the absorption resonances of 2-TP and 2-TP$^-$ has previously been shown to result from neglecting solvation effects,[8] whereas the simulated emission intensities of 2-TP$^-$ agree well with the measured spectrum. Despite the difference in absorption energy (2-TP: 400.5 eV; 2-TP$^-$: 399.0 eV), the three experimental emission features of 2-TP for an energy loss in the range of 7 to 15 eV are also observed for 2-TP$^-$ (compare Figure 2$a_1$ and $b_1$). Even the absolute intensities of these features are similar in both systems, but their shape is broader in the case of 2-TP. However, 2-TP$^-$ (Figure 2$b_1$) exhibits an additional intense emission peak at 5.2 eV energy loss, hereafter referred to as the deprotonation fingerprint.

These features can be rationalized by assignments within the molecular orbital (MO) approximation from the spectrum simulations. For both systems, X-ray excitation from the N 1s atomic orbital to an antibonding π MO causes a rehybridization of the π system in the multiconfigurational description. Emission, with varying energy loss, occurs by decay from different MOs. Several of these MOs are delocalized over the whole molecular ring. They are thus not affected strongly by the local (de)protonation, which explains the similarities in the two spectra.

The deprotonation fingerprint of 2-TP$^-$ was assigned to decay from a lone pair (LP) MO centered on the N atom. The high intensity results from strong overlap with the N 1s core orbital. In 2-TP, a N–H σ orbital is present instead of the LP orbital, which quenches the associated spectral feature. The substructure still present in the same energy loss region in Figure 2$a_1$ actually involves decay from MOs of bonding/antibonding character to the neighboring sites of the N atom.

  

Thus the fingerprint feature is a direct indication for the N site protonation state.

Focusing on the photoinduced N deprotonation process in 2-TP, we present results of time-resolved optical pump X-ray probe RIXS measurements of the VE state dynamics at the N 1s resonance, which were performed at the Linac Coherent Light Source (LCLS; see the Supporting Information for experimental details). As depicted in Figure 3a, the sample was excited with a 50 fs short laser pulse at a photon energy of 3.1 eV. A 120 fs short X-ray pulse was used to detect the ongoing VE state dynamics in 2-TP in a stroboscope-like manner by changing the X-ray photon energy and the temporal delay between the two pulses.

The integral intensity of the time-resolved RIXS measurements for incident energies in the range of the resonance of 2-TP$^-$ between 398.5 and 399.3 eV results in the spectrum presented in Figure 3b. The spectrum for positive delays ($t>0$; the X-ray pulse probes dynamics after excitation) exhibits an intensity increase in the region of 2.5 to 6.7 eV energy loss, corresponding to the previously identified fingerprint region. Thus the optical excitation gives rise to the same characteristic spectral feature as chemical deprotonation of the N atom, which was attributed to N LP orbital formation. This indicates that the initially present N–H bond is broken upon photoexcitation of 2-TP.

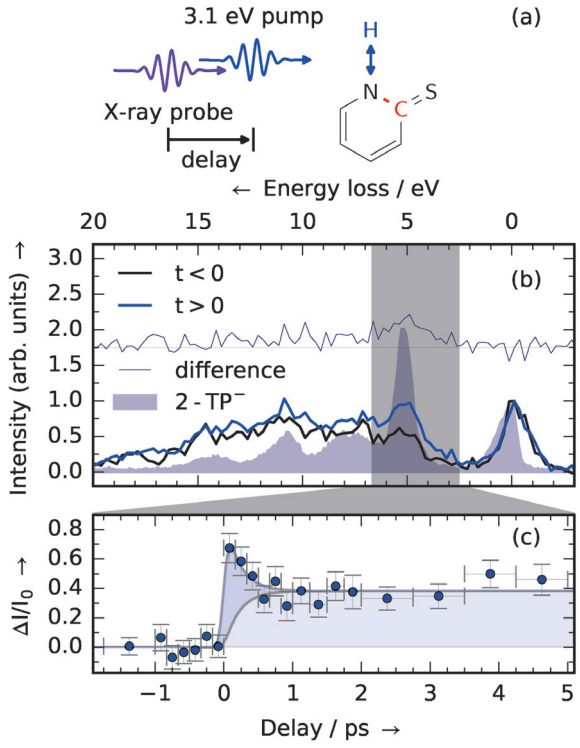


***Figure 3.*** Ultrafast initial steps of the optically induced deprotonation of 2-TP. a) Experimental concept for the detection of photoinduced N deprotonation induced by an optical pulse with a photon energy of 3.1 eV and detected with an X-ray pulse with a variable temporal delay. b) Resonant X-ray emission spectra of 2-TP before ($t<0$, −2 ps to 0 ps delay) and after ($t>0$, 0 ps to 6 ps delay) the temporal overlap of the 3.1 eV optical pump and X-ray probe pulses, their difference (offset for visualization), and the RIXS spectrum of 2-TP$^-$ from Figure 2b$_1$. Incident photon energies of 398.5 to 399.3 eV. c) Relative intensity changes in the fingerprint region of the 2-TP$^-$ species [gray region in (b), 2.5 to 6.7 eV energy loss] as function of the pump probe delay. The initial steps of the photoinduced deprotonation process were detected to occur on a timescale below the bin width of 167 fs. The fit of a rate model involving an initial, an intermediate, and a final state is displayed to indicate dynamics of the ESPT process.

Du et al. have proposed two possible pathways for photoinduced deprotonation of the N site in 2-TP via ESPT to the sulfur-protonated 2-MP species.[9] First, decay from the valence-excited 2-TP($S_2$) state [with possible relaxation into 2-TP($S_1$)] into 2-TP($T_1$) by ISC is followed by a second ISC to give 2-MP($S_0$). Second, a photoinduced proton transfer process was detected by Du et al.[9] upon 2-TP($S_4$) excitation. As an additional possible pathway, ESPT was then suggested to occur either by internal conversion into 2-MP($S_1$) or ISC into 2-MP($T_1$). Under the conditions of our experiment, the first pathway is accessible through direct excitation into the tail of the $S_2$ absorption resonance; the $S_4$ state can instead be reached by two-photon absorption. Alternatively, solvent-mediated proton abstraction, analogous to chemical detachment in our static measurements, could induce a direct deprotonation. To determine whether such sequential processes contribute to the detected deprotonation, the delay-dependent signal for incident energies between 398.5 and 399.3 eV and energy losses from 2.5 to 6.7 eV (gray region in Figure 3b) is displayed in Figure 3c. The signal increases abruptly at temporal overlap of the pump and the probe pulse. Hence, we detected the formation of a transient state on a timescale below the temporal bin width of 167 fs. Given the statistics of the presented data, it is not clear whether the slight intensity decrease within the first 500 fs after optical excitation is a signature of the details in the ongoing excited-state dynamics. Even though the formation of the intermediate state cannot be resolved, the exponential decay of the intermediate state in the rate model, consisting of a transient intermediate and a final state that is stable on the inspected timescale, with a time constant of $(0.2\pm0.1)$ ps hints towards transitions between excited states within the first few hundred femtoseconds after optical excitation. An intense emission line in the fingerprint region is a characteristic feature of all investigated species with a deprotonated N site (see the Supporting Information for further elaboration); therefore, the involved states along the deprotonation pathway cannot be uniquely assigned with the presented data, but could be identified if data with better statistics were available.

In contrast to the valence excitation, bonds within the pyridine ring of 2-TP are affected by N 1s core excitation. The varying width of the common inelastic features in the spectra between the two systems shown in Figure 2a$_1$ and b$_1$ can be correlated with different dynamics on the CE-PESs of 2-TP and 2-TP$^-$. Strong CE dynamics lead to asymmetry for both the elastic (energy loss close to zero; the RIXS final state is the electronic ground state) and inelastic (energy loss of a few eV; the RIXS final state is an electronically excited state) RIXS features in the form of vibrational progressions. The more pronounced signatures of the dynamics for 2-TP compared to 2-TP$^-$ can be conceptually understood in the $Z+1$ equivalent core approximation, wherein the CE N* is treated like a neutral oxygen atom. 2-TP$^-$ remains stable

  

because the O atom coordinates only with the C atoms in the ring. In 2-TP, the O atom is overcoordinated, which favors the cleavage of one of the bonds to the CE N site.

As the overcoordination at the N site of CE 2-TP in comparison to 2-TP$^-$ results from the presence of a proton, the N–H bond could be expected to elongate on the CE-PES, analogously to core-excitation-induced proton transfers in water and aqueous ammonia.[24,25] However, PES scans at different levels of theory (Figure 4a and b) show that the

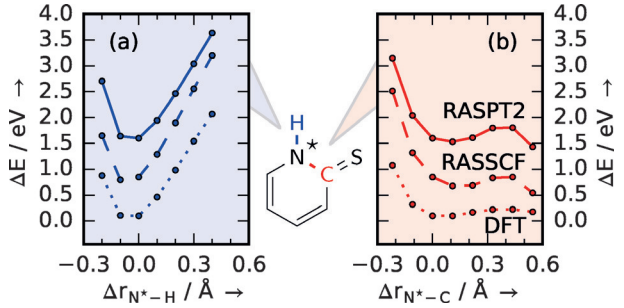


***Figure 4.*** Dynamics of N 1s core-excited 2-TP. a,b) Calculated potential energy changes $\Delta E$ of CE 2-TP as a function of the relative N*–H bond length (a, bound) and as function of the relative N*–C (b, dissociative) bond length $\Delta r$. The curves for different levels of theory are offset for visualization.

N–H (blue) coordinate remains strongly bound in the CE state. In contrast, the coordinate between N and the S-bonded C atom (red) is of dissociative character. The CE dynamics can therefore instead be ascribed to rapid N–C elongation. Focusing the investigations on scans along the N–H and N–C degrees of freedom was motivated by indications from core excited-state dynamics in DFT-based molecular-dynamics simulations. This finding is vital to the time-resolved investigation of the dynamics on the VE-PES of 2-TP as it shows that the X-ray excitation in the RIXS probe mechanism does not directly interfere with optically induced dynamics along the N–H coordinate. The two bond deformation processes are in this sense independent.

In conclusion, we have shown the capability of N 1s RIXS to detect coupled electronic and nuclear dynamics induced by excitation onto VE- and CE-PESs of 2-TP in aqueous solution on the femtosecond timescale. Through synchrotron measurements and quantum-chemical simulations, the distinct spectral signature of N deprotonation in 2-TP was identified and explained. With this fingerprint signature, ultrafast initial steps of N deprotonation induced by optical excitation were visualized in our femtosecond-resolved measurements using the X-ray free electron laser LCLS. The timescale for these steps is below 167 fs. PES simulations indicate that the distance between neighboring N and C atoms in 2-TP is selectively elongated within the femtosecond (core-hole lifetime) timescale upon X-ray excitation. Our study exemplary depicts how optical and X-ray excitation yield independent bond deformation at a specific atomic site. The identified fingerprint of deprotonation was ascribed to lone pair orbital formation, a general phenomenon that similarly occurs upon N–H bond cleavage also in other systems. N protonation states can thereby be monitored through both the chemical shifts of X-ray absorption resonances and characteristic emission channels with RIXS. This facilitates the separation of spectral signatures from multiple similar sites, indicating the applicability of RIXS to selectively trigger and detect reaction paths also in larger (bio)chemically relevant molecules.

## Acknowledgements

Technical support by Christian Weniger is thankfully acknowledged. J.N. thanks Faris Gelmukhanov for productive discussions. S.E. and A.F. acknowledge funding from the ERC-ADG-2014 (Advanced Investigator Grant 669531/EDAX) under the Horizon 2020 EU Framework Programme for Research and Innovation. S.E., J.N., W.Q., B.K., M.H., M.O., and A.P. acknowledge financial support from the Helmholtz Virtual Institute VI 419 "Dynamic Pathways in Multidimensional Landscapes". M.O. acknowledges financial support from the Swedish Research Council (VR) and the Carl Trygger Foundation. M.B. thanks the Volkswagen-Stiftung for financial support. M.R., B.V., and M.K. acknowledge the Office of Basic Energy Sciences of the US Department of Energy (Grant DE-SC0002190) for providing salary support and a David and Lucille Packard Fellowship for Science and Engineering for providing travel support. We thank the HZB for the allocation of synchrotron radiation beamtime. Use of the Linac Coherent Light Source (LCLS), SLAC National Accelerator Laboratory is supported by the US Department of Energy, Office of Science, Office of Basic Energy Sciences (DE-AC02-76SF00515). The SXR instrument is funded by a consortium that includes the LCLS, Stanford University through the Stanford Institute for Materials and Energy Sciences (SIMES), the Lawrence Berkeley National Laboratory (LBNL), the University of Hamburg through the BMBF priority program FSP 301, and the Center for Free Electron Laser Science (CFEL). The LCLS is supported by the DOE Office of Basic Energy Sciences. We thank the LCLS staff for support.

## Conflict of interest

The authors declare no conflict of interest.

**Keywords:** nitrogen · photochemistry · protonation · RIXS (resonant inelastic X-ray scattering) · selective bond cleavage

**How to cite:** *Angew. Chem. Int. Ed.* **2017**, *56*, 6088–6092
*Angew. Chem.* **2017**, *129*, 6184–6188

[1] Y. Zhang, K. de La Harpe, A. A. Beckstead, R. Improta, B. Kohler, *J. Am. Chem. Soc.* **2015**, *137*, 7059–7062.
[2] A. El Nahhas, T. Pascher, L. Leone, L. Panzella, A. Napolitano, V. Sundström, *J. Phys. Chem. Lett.* **2014**, *5*, 2094–2100.
[3] A. Corani, A. Huijser, T. Gustavsson, D. Markovitsi, P. Å. Malmqvist, A. Pezzella, M. D'Ischia, V. Sundström, *J. Am. Chem. Soc.* **2014**, *136*, 11626–11635.

  

[4] S. Olsen, J. Riesz, I. Mahadevan, A. Coutts, J. P. Bothma, B. J. Powell, R. H. McKenzie, S. C. Smith, P. Meredith, *J. Am. Chem. Soc.* **2007**, *129*, 6672 – 6673.
[5] P. Beak, J. B. Covington, *J. Am. Chem. Soc.* **1978**, *100*, 3961 – 3963.
[6] P. Beak, *Acc. Chem. Res.* **1977**, *10*, 186 – 192.
[7] P. Beak, J. B. Covington, S. G. Smith, J. M. White, J. M. Zeigler, *J. Org. Chem.* **1980**, *45*, 1354 – 1362.
[8] S. Eckert, P. Miedema, W. Quevedo, B. O'Cinneide, M. Fondell, M. Beye, A. Pietzsch, M. Ross, M. Khalil, A. Föhlisch, *Chem. Phys. Lett.* **2016**, *647*, 103 – 106.
[9] R. Du, C. Liu, Y. Zhao, K.-M. Pei, H.-G. Wang, X. Zheng, M. Li, J.-D. Xue, D. L. Phillips, *J. Phys. Chem. B* **2011**, *115*, 8266 – 8277.
[10] C. Reichardt, C. Guo, C. E. Crespo-Hernández, *J. Phys. Chem. B* **2011**, *115*, 3263 – 3270.
[11] M. Pollum, S. Jockusch, C. E. Crespo-Hernández, *J. Am. Chem. Soc.* **2014**, *136*, 17930 – 17933.
[12] M. Pollum, S. Jockusch, C. E. Crespo-Hernández, *Phys. Chem. Chem. Phys.* **2015**, *17*, 27851 – 27861.
[13] S. Mai, P. Marquetand, L. González, *J. Phys. Chem. Lett.* **2016**, *7*, 1978 – 1983.
[14] M. Pollum, C. E. Crespo-Hernández, *J. Chem. Phys.* **2014**, *140*, 071101.
[15] L. J. P. Ament, M. van Veenendaal, T. P. Devereaux, J. P. Hill, J. van den Brink, *Rev. Mod. Phys.* **2011**, *83*, 705 – 767.
[16] P. Wernet et al., *Nature* **2015**, *520*, 78 – 81.
[17] F. Gelmukhanov, H. Ågren, *Phys. Rev. A* **1996**, *54*, 379 – 393.
[18] M. Blum, M. Odelius, L. Weinhardt, S. Pookpanratana, M. Bär, Y. Zhang, O. Fuchs, W. Yang, E. Umbach, C. Heske, *J. Phys. Chem. B* **2012**, *116*, 13757 – 13764.
[19] S. Schreck, A. Pietzsch, K. Kunnus, B. Kennedy, W. Quevedo, P. S. Miedema, P. Wernet, A. Föhlisch, *Struct. Dyn.* **2014**, *1*, 054901.
[20] A. Pietzsch et al., *Phys. Rev. Lett.* **2011**, *106*, 153004.
[21] P. Å. Malmqvist, K. Pierloot, A. R. M. Shahi, C. J. Cramer, L. Gagliardi, *J. Chem. Phys.* **2008**, *128*, 204109.
[22] P. Å. Malmqvist, A. Rendell, B. O. Roos, *J. Phys. Chem.* **1990**, *94*, 5477 – 5482.
[23] F. Aquilante et al., *J. Comput. Chem.* **2016**, *37*, 506 – 541.
[24] M. Odelius, *J. Phys. Chem. A* **2009**, *113*, 8176 – 8181.
[25] L. Weinhardt et al., *Phys. Chem. Chem. Phys.* **2015**, *17*, 27145 – 27153.

Manuscript received: January 9, 2017
Revised: February 16, 2017
Final Article published: April 4, 2017

  